ELSEVIER

Nuclear Instruments and Methods in Physics Research A 402 (1998) 260–267

NUCLEAR INSTRUMENTS & METHODS IN PHYSICS RESEARCH Section A

Toward precision polarimetry of dense polarized ^{3}He targets

M.V. Romalis[d,*], P.L. Bogorad[d], G.D. Cates[d], T.E. Chupp[b], K.P. Coulter[b], E.W. Hughes[a], J.R. Johnson[e], K.S. Kumar[d], T.B. Smith[b], A.K. Thompson[c], R. Welsh[b]

[a] *California Institute of Technology, Pasadena, CA 91125, USA*
[b] *University of Michigan, Ann Arbor, MI 48109, USA*
[c] *National Institute of Standards and Technology, Gainesville, MD 20899, USA*
[d] *Princeton University, Princeton, NJ 08544, USA*
[e] *Stanford Linear Accelerator Center, Stanford, CA 94309, USA*

Abstract

We describe several new measurement and analysis techniques used to determine the polarization of the ^{3}He target in a recently completed measurement of the neutron spin structure function g_1^n at SLAC (E-154). The polarization was determined using two independent methods. The first method used a standard technique of Adiabatic Fast Passage, calibrated by a measurement of Boltzmann polarization in a sample of water. We describe several systematic effects affecting this calibration procedure. The second method used a shift of the Rb Zeeman resonance frequency due to the polarization of ^{3}He. Implementation and calibration of this technique are discussed in detail. Finally, the density of ^{3}He in the cell was measured using two independent methods, one of them based on the pressure broadening of Rb D_1 and D_2 lines due to ^{3}He.

PACS: 29.25.Pj; 33.25.+k; 33.35.+r; 25.30.Fg

1. Introduction

Nuclear spin polarized ^{3}He is used in a variety of experiments for measurements of the neutron spin structure, ^{3}He form factors, fundamental symmetry breaking tests, nuclear reactions, neutron polarizers and other applications described elsewhere in these proceedings. Many of these experiments require an accurate knowledge of the ^{3}He polarization. As the statistical error of the experiments decreases, it becomes increasingly important to control the systematic errors associated with the polarized target, its polarization, and the fraction of scattering events from the polarized gas. In this paper we describe the techniques used for polarization measurements in a recently completed SLAC experiment (E-154), which at present gives the most accurate data on the longitudinal neutron spin structure function g_1 in the deep inelastic regime.

There are several techniques that have been used for ^{3}He polarimetry. The most commonly used is an NMR technique of Adiabatic Fast Passage (AFP) [1]. Applicability of other techniques depends on the method for producing ^{3}He polarization. When ^{3}He

* Corresponding author.

0168-9002/98/$19.00 © 1998 Elsevier Science B.V. All rights reserved
PII S0168-9002(97)00847-4

is polarized by optical pumping of Rb and Rb-He spin exchange, as it was in E-154 and proposed experiments at CEBAF, one can use a frequency shift of the Rb Zeeman transition due to polarized ^{3}He [2,3]. For targets polarized using optical pumping of metastable ^{3}He, used, for example, in the DESY HERMES experiment, one can use either the polarization of one of the lines emitted by He discharge [4], or the polarization-dependent absorption of the C_9 line of metastable ^{3}He [5]. In neutron experiments, one can use the highly spin-dependent neutron absorption cross-section for measurements of ^{3}He polarization [6]. Recently, a simple technique of detecting the classical magnetic field of polarized ^{3}He has been explored [7]. Since our target used Rb–He spin-exchange for polarizing ^{3}He, we used the AFP method and the Zeeman frequency shift method. Both methods have comparable accuracy. The systematic errors in each technique are likely to come from different sources, so the agreement of the two methods makes it unlikely that a large systematic effect is unaccounted for.

Section 2 is devoted to the AFP method of polarimetry. After brief introduction of the general technique and description of the ^{3}He AFP signal, we will concentrate on the most difficult part of the measurement: the calibration of the system by detecting a known Boltzmann polarization signal from protons in water. Several systematic effects will be described in detail. In Section 3 we will describe the frequency shift method. For this experiment we developed a novel implementation of the technique. It proved robust and easy to use in an accelerator environment, and allowed on-line measurements without operator access. We will also discuss auxiliary measurements and systematic studies needed for calibration of the frequency shift data. Since both of these techniques detect a signal proportional to the density of ^{3}He, the last section will be devoted to measurements of the pressure in the cells. In addition to measuring the pressure while filling the cells with ^{3}He, we also determined it after the cells are sealed by measuring the width and shift of Rb resonance D_1 and D_2 lines.

2. NMR polarimetry

Adiabatic Fast Passage (AFP) NMR was used to measure the ^{3}He polarization at regular intervals throughout the run. This technique works in the following way. An RF field with frequency ω and magnitude $2H_1$ is applied perpendicular to a holding field H. The holding field is ramped from below the resonance, given by $H_0 = \omega/\gamma$, to above the resonance. Here γ is the gyromagnetic ratio of ^{3}He. If the sweep is adiabatic $\dot{H}/H_1 \ll \omega$, the spins follow an effective magnetic field $\boldsymbol{H}_{\text{eff}} = (H - H_0)z + H_1 x'$ in the coordinate system (x', y', z) rotating with frequency ω. The precession of the spins induces a voltage in a pick-up coil placed perpendicular to both the holding and the RF field. The voltage is detected with a lock-in amplifier synchronized to the RF frequency. For a linear ramp $H = H_0 + \alpha t$ the voltage in the coil is given by the following formula:

$$V(t) = \frac{GH_1[^3\text{He}]P}{\sqrt{(\alpha t)^2 + H_1^2}}, \tag{1}$$

where P is the polarization of ^{3}He and G is the instrumental gain of the detection system. The sweep results in the reversal of the direction of the ^{3}He polarization, but its absolute value is unchanged, provided that the spin relaxation during the sweep is negligible (fast condition). For ^{3}He this condition is expressed as $D|\nabla H_z|^2/H_1^2 \ll \dot{H}/H_1$, where D is ^{3}He diffusion constant, putting a limit on the size of the allowed field gradient. In general, it is easy to satisfy both the adiabatic and the fast condition, so the AFP losses are very small (in our case 0.1% per sweep). The signal-to-noise ratio is large and the shape of the signal closely approximates equation (1), provided that distortions due to the field gradient and lock-in time constant are small. So, in many ways this method is ideal for relative ^{3}He polarization measurements.

The main limitations for an absolute measurement is due to the uncertainty in the instrumental gain G, which depends on the geometry and gain of the pick-up coils, lock-in amplifier gain, attenuation in the cables, etc. It is usually measured by detecting an AFP signal from a sample of known Boltzmann polarization. Water is usually used because it has one of the highest concentration of protons. There are several factors which make this calibration difficult. The AFP signal from a water sample is 10^5 times smaller than the ^{3}He signal because the thermal polarization of water $P = \mu_p H/k_B T = 7.5 \times 10^{-9}$ at typical holding fields. The signal to noise ratio is poor, and one usually

has to resort to averaging to measure the water signal with desired accuracy. In our case, each set of water data consisted of about 50 sweeps. Second, the relaxation times in water are much shorter than in ^{3}He, and the fast condition for negligible relaxation during the sweep cannot be fully satisfied. As a result, the signal shape is significantly different from (1) and requires careful analysis. Third, the sample used for water calibration usually has slightly different dimensions and position relative to the pick-up coils compared the ^{3}He cell, and these differences have to be corrected for. Finally, the water calibration is a time consuming procedure and consequently is done infrequently. So, one has to insure the stability of the system gain G between the measurements. We will only address the questions of thermal relaxation and corrections due to different dimensions, because our methods and results have applicability beyond our own experiment.

The fast condition for water AFP is different from ^{3}He AFP because the polarization is proportional to the magnetic field and can change during the field sweep. Therefore, the polarization will stay constant during the entire sweep only if $T_s \ll T_1$, where T_s is the total sweep time and T_1 is the longitudinal nuclear spin relaxation, which is on the order of 2 sec. It is difficult to satisfy this condition for a variety of reasons. Therefore, we have to take the relaxation during the sweep into account. We use the Bloch equations to describe the time evolution of the three components of the polarization (P_x, P_y, P_z) in the rotating frame [1]:

$$\begin{aligned}
\frac{dP_x}{dt} &= \gamma P_y(H - H_0) - \frac{(P_x - \chi H_1)}{T_2(H_1)}, \\
\frac{dP_y}{dt} &= -\gamma P_x(H - H_0) + \gamma P_z H_1 - \frac{M_y}{T_2(H_1)}, \\
\frac{dP_z}{dt} &= -\gamma P_y H_1 - \frac{(P_z - \chi H)}{T_1},
\end{aligned} \tag{2}$$

where T_1 is the longitudinal relaxation time, $T_2(H_1)$ is the transverse relaxation times in the presence of the rotating magnetic field H_1, and $\chi = \mu_p/k_B T$. Relaxation during the sweep affects both the height and the shape of the AFP signal. It also makes the signal dependent on the speed and direction of the magnetic field sweep.

The longitudinal relaxation time is very sensitive to the temperature and chemical purity of water. It is also affected by the presence of dissolved oxygen, which is paramagnetic [8]. At 20°C the relaxation time in water free from dissolved oxygen is 2.95 ± 0.1 s [9]. It changes by 0.4 s if the temperature is changed by 5°C. If the water is saturated with dissolved oxygen, the relaxation time is 2.2 s at 20°C. In our calibration we used deionized but not de-oxygenated water, which had a $T_1 = 2.4 \pm 0.3$ s. The relaxation time was measured in situ by comparing the height of the water signal from the up and down sweeps through the resonance.

Naively, one would expect that $T_2 = T_1$ for water since the correlation time, τ_c, associated with the translation and rotation of the molecules is much shorter than the Larmor frequency [1]. However, several measurements [10–12] show that

$$1/T_2 = 1/T_1 + 0.125\ \mathrm{s}^{-1} \tag{3}$$

for neutral (i.e. pH = 7.0) water. The reason for this turns out to be the presence of 0.037% of ^{17}O isotope in natural water [11]. ^{17}O has a nuclear spin of $\frac{5}{2}$ and an effective scalar coupling to proton spins. The time that an H atom spends attached to a particular water molecule with an ^{17}O is about 10^{-3} s. The relaxation time of the ^{17}O spin itself is about 4×10^{-3} s. Since neither of these times is shorter than the Larmor frequency ω, the motional narrowing does not apply. As a result, the proton resonance is split into several lines and the transverse relaxation time is reduced compared to the longitudinal relaxation time. In addition to ^{17}O, there are also some paramagnetic ions [11,13] which can form molecular complexes with water and reduce the value of T_1 and T_2 by different amounts. We have measured T_1 and T_2 of our sample using a pulsed NMR system. T_1 was measured by saturation recovery and T_2 using a CMPG spin-echo sequence [14]. Our results are in agreement with Eq. (3) and exclude additional contamination by paramagnetic ions. Finally, to calculate the value of $T_2(H_1)$ in the presence of the rotating field we use $H_1 = 0.086$ G and results from [11] to get $T_2(H_1) = 2.2$ s.

To extract a signal height from the water data, it is convenient to have an analytic functional form which can be used to fit the data. By solving Eqs. (2) numerically, we found that if the difference between T_1 and T_2 is not very large, the signal shape is well approximated by setting $T_1 = T_2$. However, the height of the signal is reduced (in our case by 0.4%) due to $T_2 < T_1$.

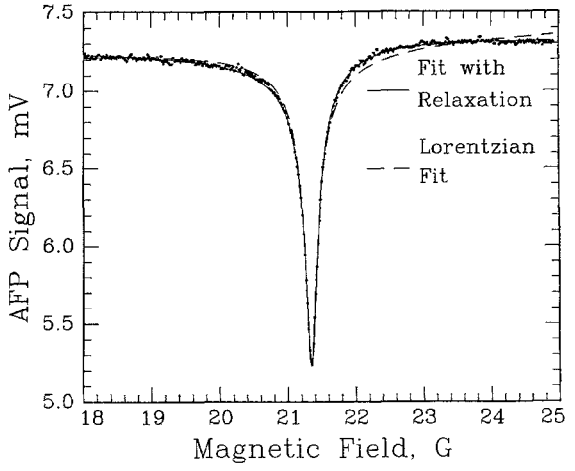

Fig. 1. An average of 50 water signals. The solid line is a fit to the signal shape (4) which takes relaxation during the sweep into account, the broken line is a fit to a simple lorentzian shape (1).

This correction can be applied separately. For $T_1 = T_2$ Eqs. (2) are reduced to a single equation for P_{eff} directed along the effective field:

$$\frac{dP_{\text{eff}}}{dt} = \frac{1}{T_1}(P_{\text{eq}}(t) - P_{\text{eff}}),$$

$$P_{\text{eq}}(t) = \chi\left(\frac{H(H-H_0)+H_1^2}{\sqrt{H_1^2+(H-H_0)^2}}\right). \quad (4)$$

It still cannot be solved analytically, however, it involves only a single integration. Furthermore, if $H_1/\alpha \ll T_1$, one can expand the resulting integral in powers of t/T_1 near the resonance and powers of $\alpha t/H_1$ away from the resonance, and get an analytic, but cumbersome, function for the signal. This method was used in our analysis. Fig. 1 shows an averaged water signal with a fit based on Eq. (4). A simple fit to Eq. (1) is also shown for comparison. In each case we vary five parameters: the height, width, and center of the peak, as well as a linear background. By using a functional form that closely approximates the shape of the signal, we are reducing the sensitivity of the final result to small distortions caused by background fluctuations, etc. The residuals of the fit are consistent with random noise. The signal heights extracted from the sweep up through the resonance and down through the resonance are consistent within errors. In contrast, if one uses a simple fit in the form (1), the two heights are different by 20%. The average of the two heights requires a correction on the order of 1%. Our final result for the water signal height has a 1% statistical uncertainty, and a conservative 1.5% systematic error.

Another set of corrections required for water calibration are associated with geometrical differences between the ^{3}He cell and the water cell. The corrections may be due to slightly different shape or dimensions of the two cells, different position between the coils and other miscellaneous effects. In some cases, the corrections are as large as 20%, because the signal scales with the volume of the cell. For our experiment, we found that the best way to handle these corrections is by using a complete coil model. Otherwise, the mutual correlation of different effects can cause changes in the result on the order of 2–3% depending on how the corrections are applied.

The signal induced in the coil is proportional to the flux of the magnetic field created by the spins through the pick-up coil. The calculation can be substantially simplified by using the law of mutual inductances to show that the flux is proportional to the average magnetic field of the pick-up coil over the volume of the cell. Furthermore, by using vector indentities we can reduce the integration to a two-dimensional integral of the pick-up coil vector potential over the surface of the cell. Our model included all aspects of the cell geometry and the finite thickness of the coil winding. Nevertheless, the calculations are simple enough to be performed on Mathematica. To check the accuracy of the coil model, we compared the predicted size of the water signal with the measured signal. The results are within 3% of each other, while the error of the model calculation is about 5%, mainly due to uncertainty in coil dimensions. Thus, the calculations of the coil response can serve as a powerful systematic check.

The final error of our AFP polarimetry is 3.4% which comes in roughly equal proportions from uncertainties in the height of the water signal, ^{3}He density, dimensions and position of the cell, temperature of the water cell, and several other sources.

3. Zeeman frequency shift polarimetry

The second method of polarimetry uses a shift of the Rb Zeeman resonance (EPR) frequency due

to the polarization of ^{3}He. It is shifted due to the Rb-He spin exchange interaction, and also due to the classical magnetic field created by polarized ^{3}He. The effect of the Rb-He spin exchange can be described by an additional magnetic field experienced by the Rb atoms:

$$B_{SE} = (2K_{He}\langle v\sigma_{SE}\rangle/g_s\mu_B)[^3\mathrm{He}]P, \quad (5)$$

where K_{He} is a parameter characterizing the size of the frequency shift [15], $\langle v\sigma_{SE}\rangle$ is the velocity averaged Rb–He spin exchange cross section, $g_s \approx 2$ is the electron g factor, and μ_B is the Born magneton. In addition, there is a shift of the Zeeman frequency due to a classical magnetic field created by polarized ^{3}He: $B_M = C\mu_{He}[^3\mathrm{He}]P$, where μ_{He} is the ^{3}He magnetic moment, and C is a constant that depends on the geometry of the sample. Both shifts are proportional to the polarization and density of ^{3}He, and they can be combined for a sample of specific shape. For a spherical sample, one defines a single constant κ_0 through the following relation [2]:

$$B_{He} = (8\pi/3)\kappa_0\mu_{He}[^3\mathrm{He}]P. \quad (6)$$

We note that classically $\kappa_0 = 1$, so it can be thought of as an enhancement factor due to attraction of the Rb electron wave function to the ^{3}He nucleus. The magnetic field causes a shift of the Zeeman resonance $\Delta\nu_{He} = (d\nu_{EPR}(F,M)/dB)B_{He}$, where $d\nu_{EPR}(F,M)/dB$ is given by well-known Breit–Rabi equation. Here F and M are the quantum numbers of the Rb hyperfine manifold. The size of the shift is large (in our case about 20 kHz), and can be easily detected in a typical field of 20 G, where the Rb Zeeman frequency is 9.3 MHz.

We detected the frequency of the resonance optically, by monitoring the fluorescence while optically pumping the cell. The intensity of the fluorescence emitted from the cell during optical pumping is proportional to the rate of photon absorption in the cell. When the Rb vapor is highly polarized, most of the ^{85}Rb atoms are in $F = 3$, $M = 3$ state, and unable to absorb photons due to angular momentum selection rules. By applying an RF magnetic field at the frequency corresponding to $M = 3 \rightarrow 2$ transition we can transfer some atoms to $M = 2$ state, where they can absorb the photons from the pumping lasers. This increases the intensity of the fluorescence, which is detected by a photo-diode.

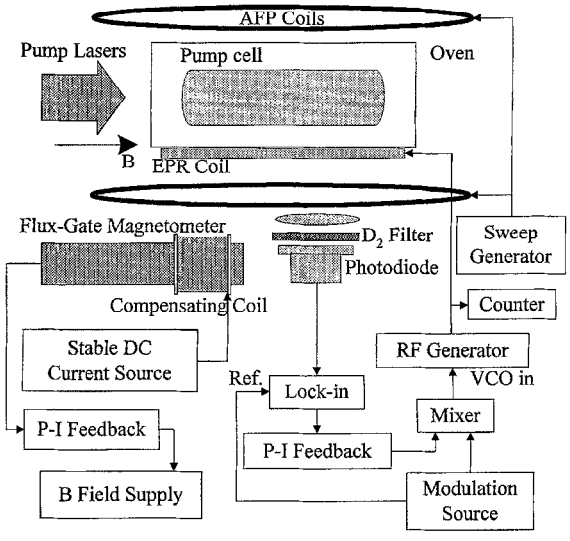

Fig. 2. Equipment setup for the EPR detection and measurement of the frequency shift.

The equipment setup for EPR measurements is shown in Fig. 2. The RF field was created by a coil mounted on the side of the oven. The fluorescence from the cell was detected by a photodiode with a D_2 filter to block the scatter from the pumping lasers. The frequency of the RF field was modulated using a Voltage Controlled Oscillator (VCO). The signal measured by the lock-in amplifier referenced to the modulation frequency was proportional to the derivative of the resonance line shape. The feedback circuit adjusted the DC level at the input of the VCO to keep the lock-in signal zero, i.e. locked to the center of the line. The RF frequency was measured by a counter and recorded by a computer. To accurately determine a shift in the Zeeman resonance frequency it was important to keep the magnetic field stable to one part in 10^5. We used a Bartington flux-gate magnetometer to measure the magnetic field. Since the range of the magnetometer is only -5 to 5 G, we cancelled the holding field by a small coil wound around the magnetometer. The field and the field gradient created by the coil near the target were negligible. The coil was driven by a stable current source that served as a reference to which the holding field was locked. The output of the magnetometer was kept near zero by a feedback circuit controlling the power supply for the Helmholtz coils.

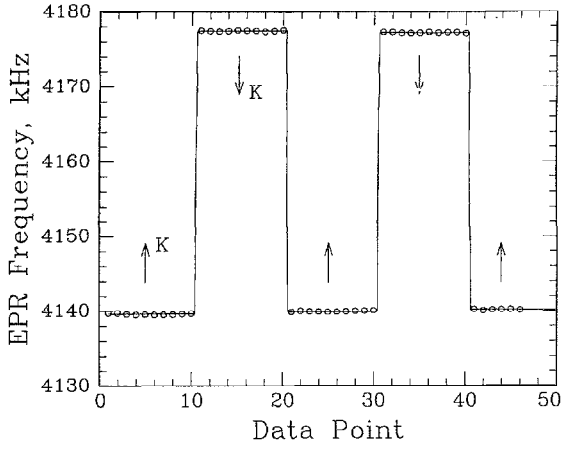

Fig. 3. A typical measurement of the frequency shift.

To isolate the frequency shift due to the ^{3}He polarization we periodically reversed the direction of the polarization. The reversal was done by AFP, only instead of sweeping the magnetic field through the resonance we swept the RF frequency. The behavior of the spins during the frequency sweep AFP is identical to the field sweep AFP, and the end result of the sweep is an 180° flip. We utilized the same coils, RF amplifier and generator as used for NMR polarimetry. The measurement cycle consisted of recording the EPR frequency for about 1 min, then flipping ^{3}He spins by AFP and recording the frequency for another minute. This procedure was repeated several times. A typical data set is shown in Fig. 3. The data are fit allowing a small amount of polarization loss per cycle, which is due to the AFP losses and the decay of the polarization during one half of the cycle when the lasers are pumping in the direction opposite to the ^{3}He polarization. The quality of the data is very good and the size of the frequency shift can be extracted with an error of less than 0.5%.

To use this data for polarimetry we need to know the value of κ_0. Unlike the gain of the NMR coil, it is a constant of the Rb-He spin exchange process, and depends only on temperature. Although it was measured previously [16,17], none of the measurements were done at high temperature and Rb number density used in our experiment. Therefore, a new experiment was done under typical conditions of optical pumping [18]. The measurement used an interplay between the spin-exchange and classical magnetic field shifts of the Zeeman resonance [17] and was, in essence, self-calibrating. We get the following result $\kappa_0 = 4.52 + 0.00934\,\mathrm{T}$ (°C). The error on κ_0 at 170°C is 1%. The measured slope agrees very well with a previous result [16]. Using this slope we can also compare our number with the previous measurement [17], which has a error of 2.5% and was done at much lower temperature. The results are within 1.6% of each other.

Two corrections have to be applied to the frequency shift data. The target pumping cell, where the measurements were performed, was not spherical, so a small additional shift due to the classical magnetic field should be added to Eq. (6). It results in a 4.6% correction and a 1.3% error. The error is due to our limited knowledge of the region in the pumping cell which was sampled by the photo-diode.

The frequency shift measures the polarization of ^{3}He in the pumping chamber of the cell. There is a small polarization gradient between the pumping and target cells due to a finite diffusion time. It results in a 3.8% correction and a 1.5% error. The correction was calculated by using a model of diffusion between the target and the pumping cells. The model was checked by measuring the polarization build-up in the target cell in the first hour of spin-up. The error is due to the uncertainty in target spin relaxation rates.

The total error of the frequency shift polarimetry method is 3%, coming from the uncertainty in the value of κ_0, the density of ^{3}He, and the two corrections described above.

4. ^{3}He density measurements

Since the density of ^{3}He is common to both polarimetry techniques, we measured it in two independent ways. As usual, we calculated the density using pressure measurements during the filling of the cells with an accuracy of 1%. While the accuracy of this method is sufficient, the measurements cannot be rechecked for errors and the possibility of cell leakage after filling cannot be excluded. Therefore, the cell density was also measured using a different technique that allows the measurements to be done after the cells have been filled and sealed. It uses the broadening and shift of the Rb resonance absorption lines

Table 1
Specific broadening and shift of Rb D_1 and D_2 resonance lines in the presence of ^{3}He. The constants are defined in the text

	Γ_0 (GHz)	a (GHz/amg.)	ν_0 (GIIz)	b (GHz/amg.)	c (GHz/amg.^{2})
D_1	0.46	9.34	1.21	4.97	0.141
D_2	0.08	10.38	0.48	0.583	0.0415

by ^{3}He. In the presence of several atmospheres of He gas, the pressure broadening of the Rb absorption lines, D_1 and D_2, exceeds the Doppler broadening and the lines acquire a simple lorentzian shape [19]: $\sigma(\nu) = \sigma_0\Gamma/((\nu - \nu_c)^2 + \Gamma^2)$. As was first measured by Chen [20], the width and the shift of these lines is approximately linear in He pressure to several tens of atmospheres and can serve as a good measure of the He density. In a separate experiment [21] we studied the pressure dependence of the line widths and shifts. It is well described by a linear fit $\Gamma = \Gamma_0 + a[^3\mathrm{He}]$ for the width and quadratic fit for the center: $\nu_c = \nu_0 + b[^3\mathrm{He}] + c[^3\mathrm{He}]^2$. The results are shown in Table 1. The density was determined from three different quantities: the width of D_1 and D_2 lines, and the shift of D_1 line (the shift of D_2 line is too small for accurate measurements). A small correction was applied to take into account the presence of N_2 in the cells. The errors are approximately 2.5% for density determined from D_1 width, 1.5% from D_2 width and 1.7% from D_1 shift, which are determined from the scatter of the data for different cells. All four methods of measuring ^{3}He density are in good agreement with each other.

5. Conclusions

The polarization of ^{3}He was measured by two independent methods, using Adiabatic Fast Passage and Rb Zeeman frequency shift. The uncertainties are 3.4% for the AFP method and 3.0% for the frequency shift method. The results of the two methods differ by 5.4%. Since the errors in each method come from many independent sources, we are justified to combine them in quadrature. The difference is 1.2 times larger than the combined error of the two measurements. Thus, the two methods are in agreement.

In conclusion, we described the two methods of ^{3}He polarimetry used in E-154. For the AFP method we considered in detail the effect of thermal relaxation of protons in water. We also described a novel implementation of the Zeeman frequency shift polarimetry suitable for a nuclear physics experiment. Because this technique was used for the first time, several refinements are still possible. The uncertainty due to the classical magnetic field shift can be reduced by restricting the region of the cell sampled by the photodiode. The error due to finite diffusion time between cells can be reduced by making special measurements designed to study the effect. Because the technique relies on a frequency shift, which can be measured with very high accuracy, we believe that with these refinements the error can be reduced below our value of 3%.

Acknowledgements

We would like to thank Prof. M. Tanaka for an invitation to present this work at the workshop. One of us (MVR) would like to thank Prof. William Happer for many useful discussions. This work was supported by the Department of Energy contracts: DE-AC03-76SF00515 (SLAC), DE-FG02-90ER40557 (Princeton) and by an NSF Grant 9217979 (Michigan).

References

[1] A. Abragam, Principles of Nuclear Magnetism, Oxford University Press, 1961.
[2] S.R. Schaefer, G.D. Cates, T.R. Chien, D. Gonatas, W. Happer, T.G. Walker, Phys. Rev. A 39 (1989) 5613.
[3] N.R. Newbury et al., Phys. Rev. Lett. 67 (1991) 3219.
[4] W. Lorenzon, T.R. Gentile, H. Gao, R.D. McKeown, Phys. Rev. A 47 (1993) 468.
[5] N.P. Bigelow, P.J. Nacher, M. Leduc, J. Phys. II, 2 (1992) 2159.
[6] G.L. Greene, A.K. Thompson, M.S. Dewey, Nucl. Instr. and Meth. A 356 (1995) 177.
[7] E. Wilms, M. Ebert, W. Heil, R. Surkau, preprint, 1996.

[8] G. Chiarotti, G. Cristiani, L. Giulotto, Nuovo Cimento 1 (1955) 863.
[9] J.H. Simpson, H.Y. Carr, Phys. Rev. 111 (1956) 1201.
[10] S. Meiboom, Z. Luz, D. Gill, J. Chem. Phys. 27 (1957) 1411.
[11] S. Meiboom, J. Chem. Phys. 34 (1961) 375.
[12] R.E. Glick, K.C. Tewari, J. Chem. Phys. 44 (1966) 546.
[13] R. Hauser, G. Laukien, Z. Physik 153 (1959) 394.
[14] E. Fukushima, S.B.W. Roeder, Experimental Pulse NMR, Addison-Wesley, 1993.
[15] L.C. Balling, R.J. Hanson, F.M. Pipkin, Phys. Rev. 133 (1964) A607.
[16] N.R. Newbury, A.S. Barton, P. Bogorad, G.D. Cates, M. Gatzke, H. Mabuchi, B. Saam, Phys. Rev. A 48 (1993) 558.
[17] A.S. Barton, N.R. Newbury, G.D. Cates, B. Driehuys, H. Middleton, B. Saam, Phys. Rev. A 49 (1994) 2766.
[18] M.V. Romalis et al., to be published.
[19] C. Ottinger, R. Scheps, G.W. York, A. Gallagher, Phys. Rev. A 11 (1975) 1815.
[20] S.Y. Ch'en, Phys. Rev. 58 (1940) 1051.
[21] M.V. Romalis, E. Miron, G.D. Cates, to be published.